1 Model evaluation for Technology F

1.1 Device information

The provided device is a double-poly self-aligned epitaxial base transistor fabricated in a BiC-MOS foundry process. It is the high-speed transistor version with a SIC. The transistor size is $0.4*2\mu m^2$ with a 111 contact configuration.

- The provided data consists of
  - de-embedded S-parameters as a function of frequency for V_{BC} = const(various values) as well as a function of bias at a single frequency f = 2 GHz; temperature T = 23.2C is given as information in some file headers.
  - DC bias data, measured on the same device type, but not the *same* device, for V_{BC} = const(various values).

1.2 Parameter extraction

Since S-parameter (AC) and DC measurements were taken for different transistors (even if the type is the same), DC bias differs from AC bias data: in this case, IC data show up to 46%, IB data show up to 16% deviation between the data sets. This is shown in Fig. 1.2/1. Also, C_{BC} capacitance data not only showed up to about 20% differences depending on the y-parameter data used but also a different voltage dependence. Nevertheless, the respective capacitance curve can be approximated sufficiently well by HICUM as Fig. 1.2/2 demonstrates. In contrast to C_{BC}, C_{BE} data show very large variation and were, therefore, adjusted directly based on y-parameters and $1/(2\pi f_T)$ measurement data.

Due to the mentioned inconsistencies, it is impossible to obtain a *single* set of model parameters that accurately describes the characteristics obtained from DC and AC measurements. Therefore, the parameter extraction was performed using each consistent set of data, starting with the AC data set. It turned out that most of the extracted parameters seemed also to be applicable to the DC data set, except few ones.

However, the availability of such limited data leads to an even more under-determined extraction problem and further increases the difficulty obtaining physics-based parameter values. For instance, the I-V_{BE} characteristics at high current densities are influenced simultaneously by series resistances (mostly r_E and r_B), self-heating (R_{th} in combination with E_g and TCs); in addition, the avalanche current and its temperature dependence enter the I_B curve while high-current effects and associated temperature effects enter the I_C curve which in turn affects the I_B curve through the series resistances and the modulation of r_{Bi}. Another example is the *accurate* determination of the minority charge that requires the knowledge of r_{Cx} and r_E as well as of the *separate* bias dependence of the *internal and external portion of the BC depletion capacitance* which is impossible with the provided subset of consistent AC data from just a single device.

Data for a possible substrate transistor action was not available. However, available DC data from both AC and DC measurements do not show substrate transistor action.

Below, first the results obtained for the AC data set are shown, followed by the results for the DC data set (and additional comments). In many cases the data are plotted vs. the (log of) collector current density I_C/A_E rather than vs. V_{BE}. The latter is of little interest and use for circuit design, and does not provide circuit design related information on the bias point. Note, that $V_{BE} \sim \log(I_C)$ for low current densities.

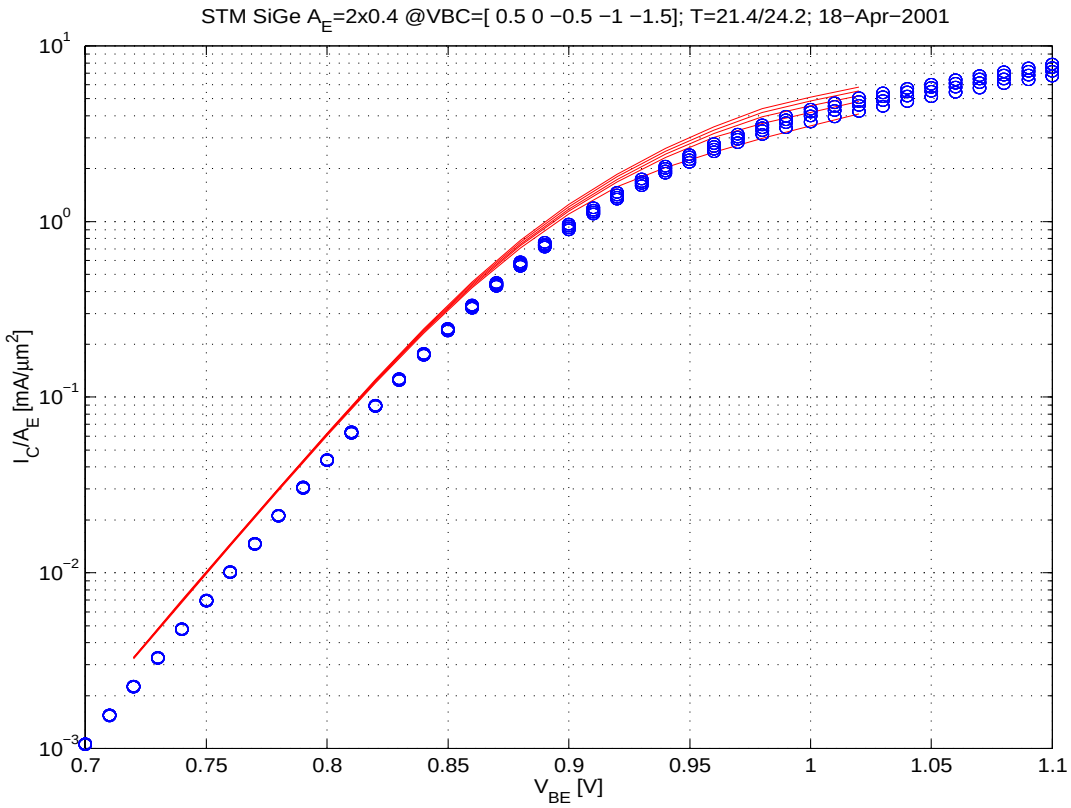

Fig. 1.2/1: Collector current in [A] vs. V_{BE} in [V] for DC data from AC and DC measurements, showing the difference between the data sets.

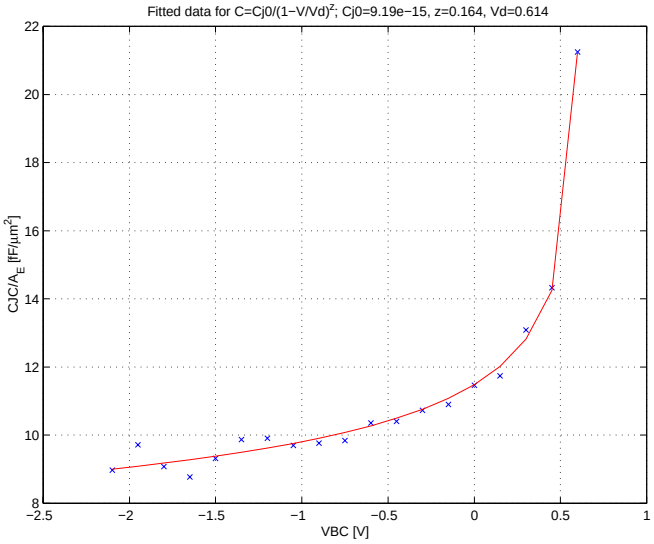

Fig. 1.2/2: HICUM approximation (line) of one of the BC capacitance data sets (symbols).

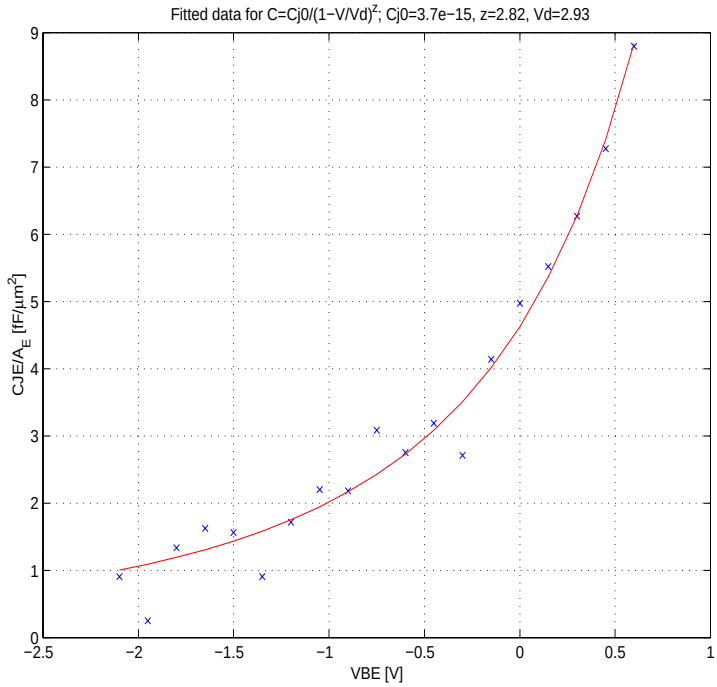

Fig. 1.2/3:HICUM approximation (line) of one of the BE capacitance data sets (symbols).

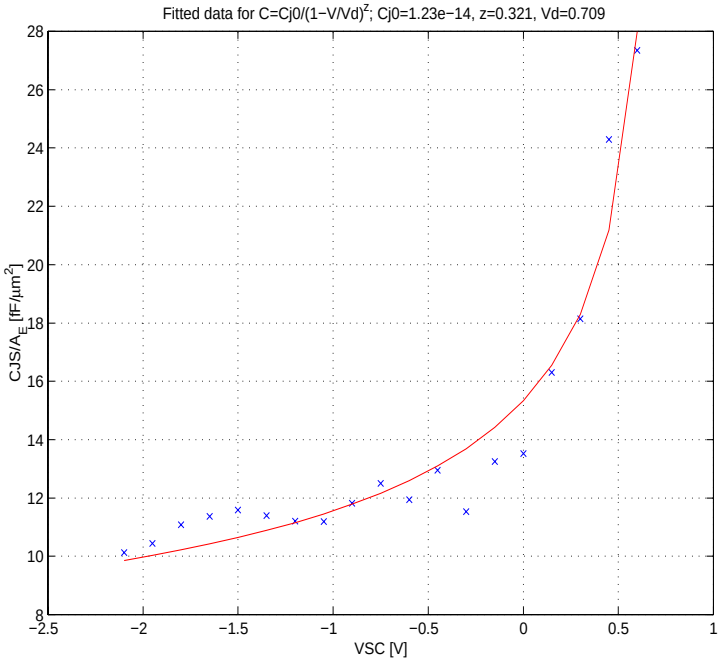

Fig. 1.2/4:HICUM approximation (line) of one of the substrate capacitance data sets (symbols).

1.3 Results for the AC measurement data

Figures 1.3/1 to 1.3/4 contain a comparison of standard characteristics between model (solid lines) and measurements (symbols). In detail, while the collector current shows very good agreement over the whole bias range, some deviations can be observed in I_B at high current densities beyond peak f_T. These deviations can be caused by uncertainties in, e.g., (a) Q_{p0} (and geometry partitioning of depletion charges), (b) series resistances, (c) self heating and temperature coefficients, and (d) geometry partitioning of the minority charge and associated current dependence (although the latter could be kept small due to the availability of f_T data).

Fig. 1.3/5 shows the y-parameters as a function of collector current density at f = 2GHz and constant V_{BC} values.

Figures 1.3/6 to 1.3/9 contain comparisons of frequency dependent y-parameters for selected bias points. In the first two figures, a set of curves was picked for V_{BC} = 0.5V, which is an extreme case, especially at high current densities: Fig. 1.3/7 shows fairly good results even for a current density, that is about 25% beyond the one where f_T peaks. (Note that the model was simulated up to 20GHz while measured data was available up to 18GHz.) In the last two figures, the curves were selected for the highest available (reverse) voltage V_{BC}=-1.5V in order to demonstrate the capability of HICUM to cover a larger bias range without loss of accuracy. For both voltages, the agreement at the lower current densities (Figs. 1.3/6 and 1.3/8) is also quite good.

At low frequencies, the measurement uncertainty does not always allow a clear conclusion. The deviations in $\mathrm{Re}\{y_{22}\}$ might be caused by substrate coupling, which might be more complicated for the investigated transistor than the simple RC network in HICUM is capable of modeling.

In summary, all characteristics show good to reasonable agreement up to peak f_T.

The combination of model parameter values found during fitting (cf. Fig. 1.3/10) describes the characteristics in the operating regions of interest reasonably well, but can be improved by both an independent determination of, e.g., series resistances and geometry effects, and the availability of additional *consistent* capacitance data.

Note:

- f_T peaks - depending on V_{BC} - between J_C values of 0.8 and 2 mA/μm^2;
- operation beyond peak f_T is of interest only for circuits switching at high-speed, in which the dynamic base current can be much larger than the DC base current, making accurate DC base current modeling irrelevant compared to accurate modeling of charges which is reflected by f_T and in some cases also by, e.g., f_{max}.

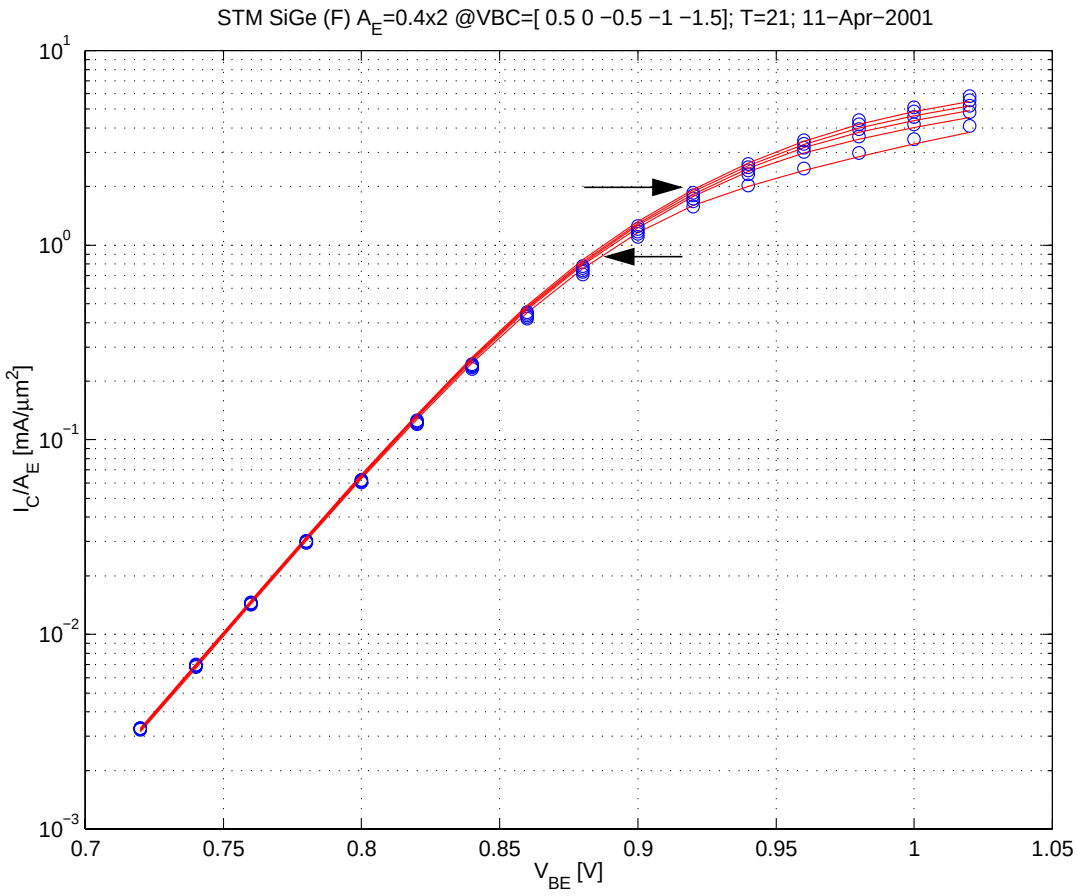

Fig. 1.3/1: Collector current density vs. V_{BE} for V_{BC}/V = 0.5, 0, -0.5, -1, -1.5. Data source: AC measurements.
The arrows indicate peak f_T for the lowest and highest V_{BC} value.

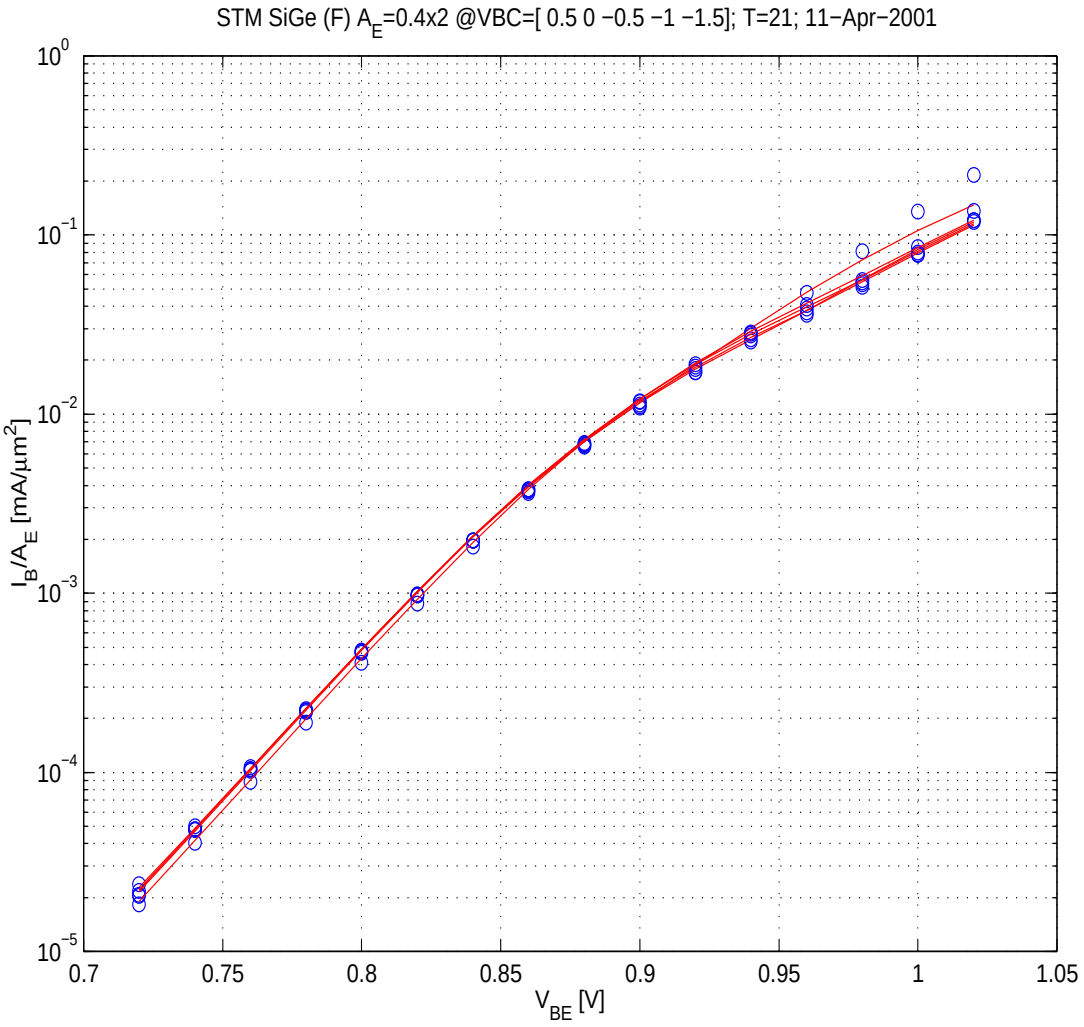

Fig. 1.3/2: Base current density vs. V_{BE} for V_{BC}/V = 0.5, 0, -0.5, -1, -1.5. Data source: AC measurements.

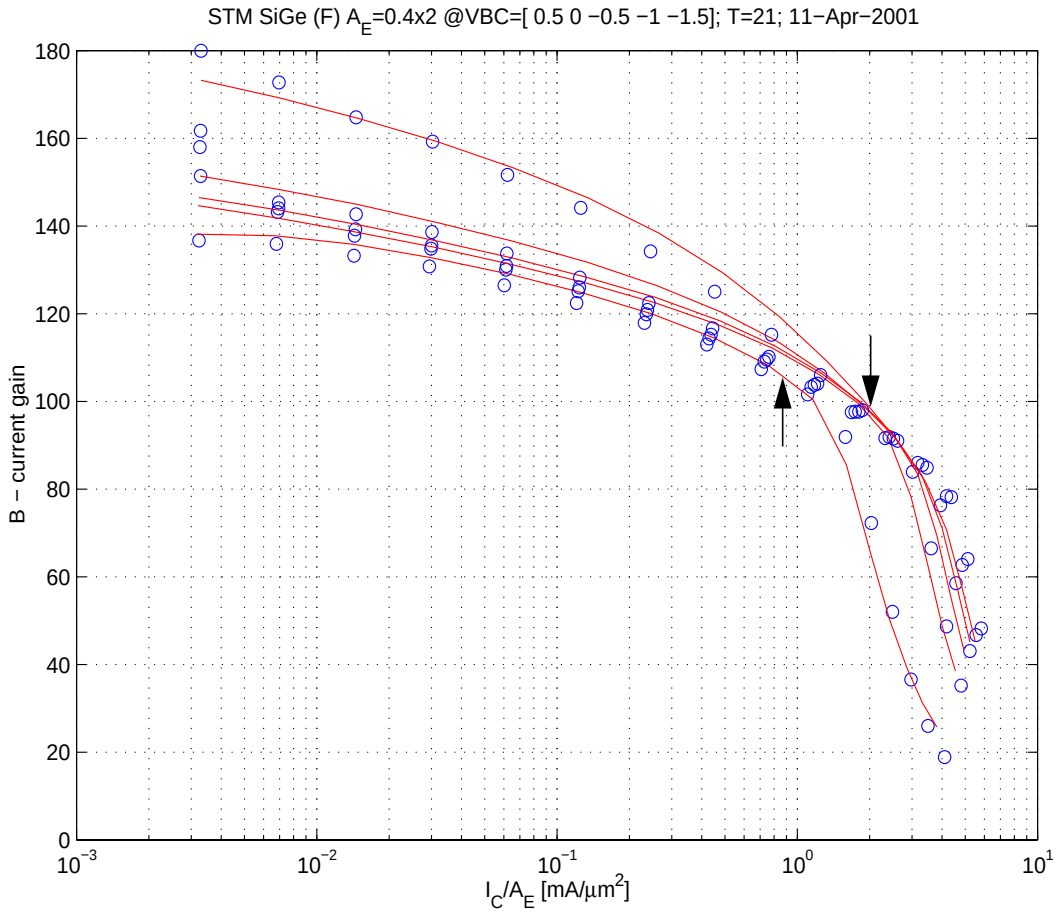

Fig. 1.3/3: DC current gain vs. collector current density for V_{BC}/V = 0.5, 0, -0.5, -1, -1.5. Data source: AC measurements.
The arrows indicate peak f_T for the lowest and highest V_{BC} value.

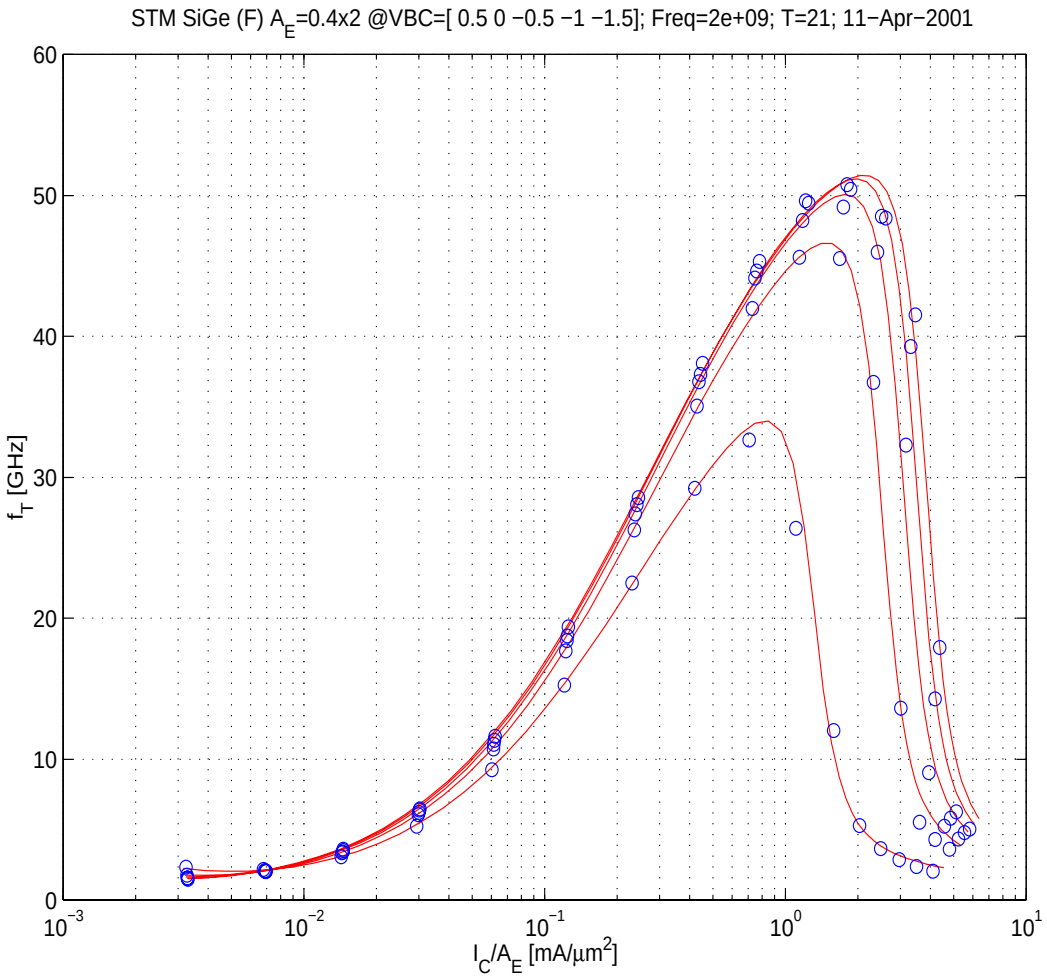

Fig. 1.3/4: Transit frequency vs. Collector current density for V_{BC}/V = 0.5, 0, -0.5, -1, -1.5.

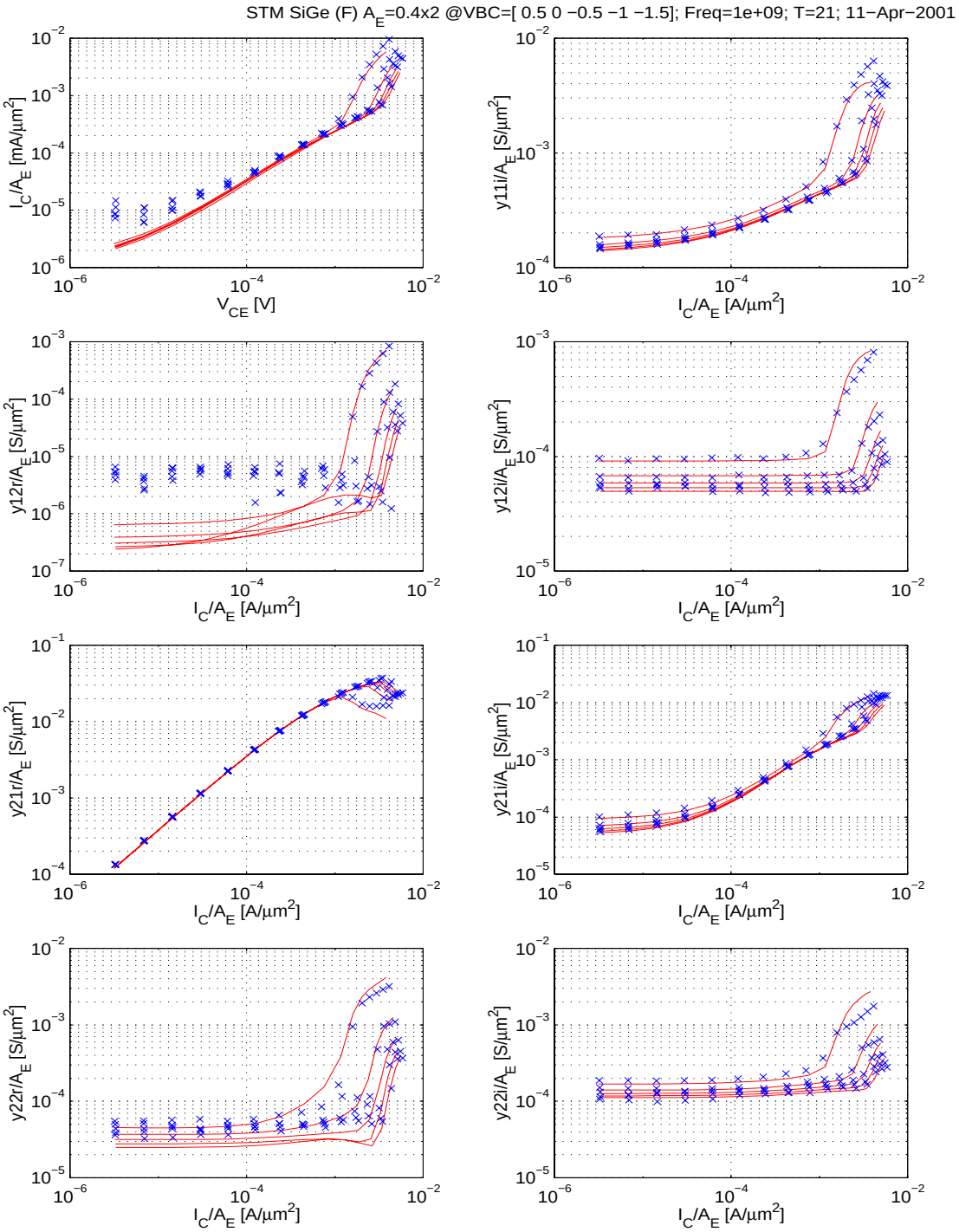

Fig. 1.3/5: Bias dependent y-parameters for f = 1GHz; V_{BC}/V = 0.5, 0, -0.5, -1, -1.5.

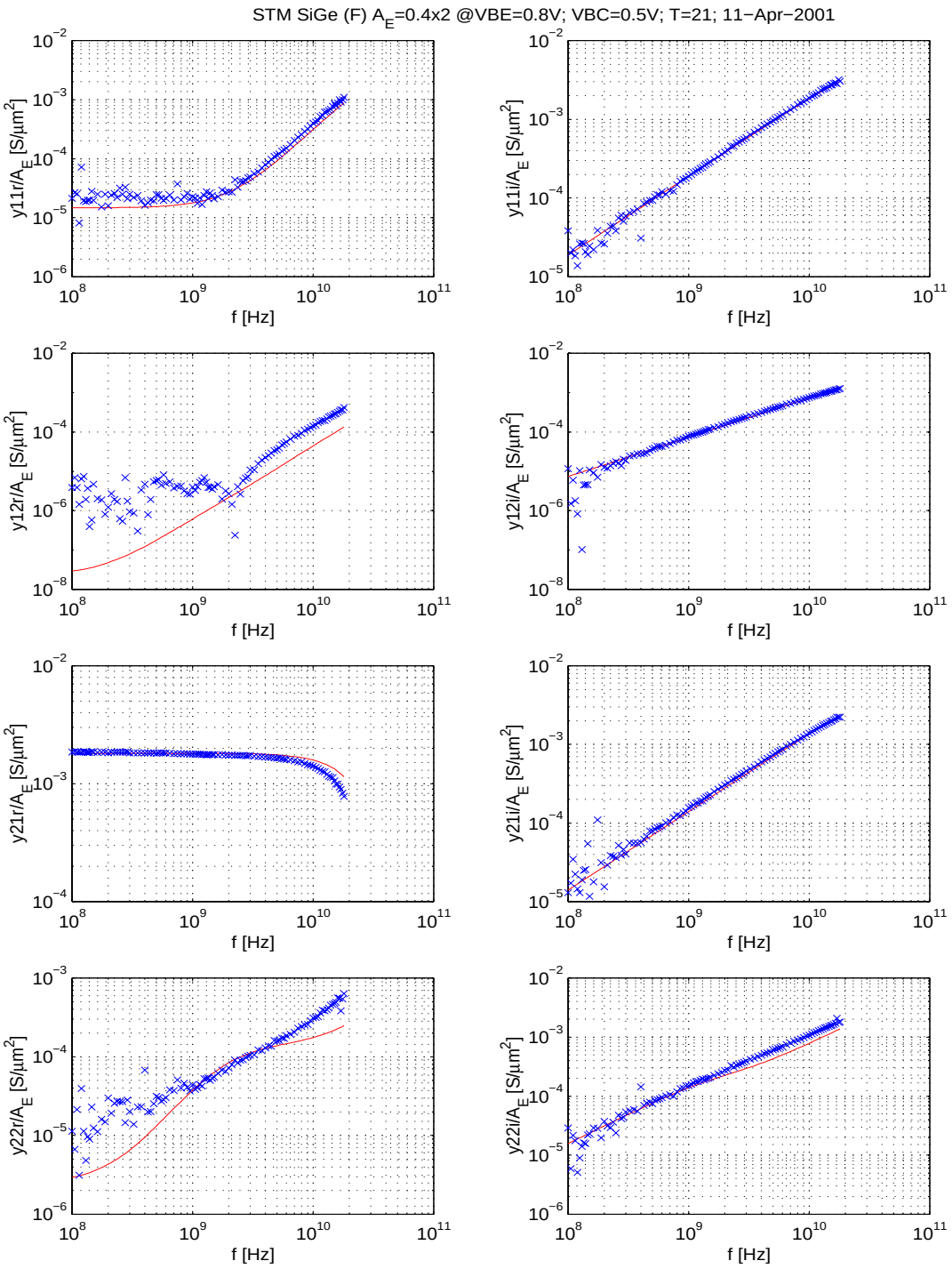

Fig. 1.3/6: Frequency dependent y-parameters at V_{BC} = 0.5V and I_C/A_E below peak f_T.

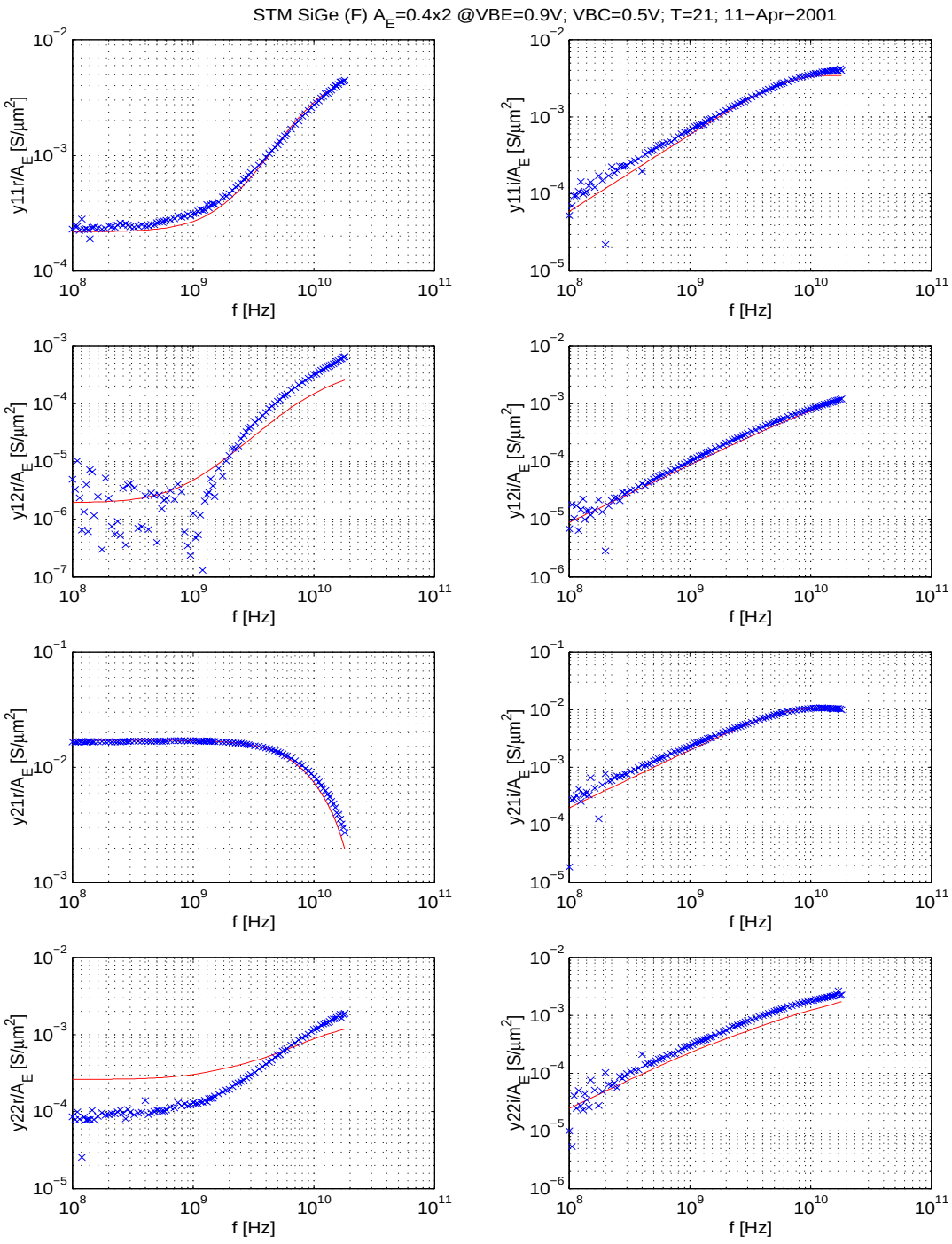

Fig. 1.3/7: Frequency dependent y-parameters at V_{BC} = 0.5V and I_C/A_E above peak f_T.

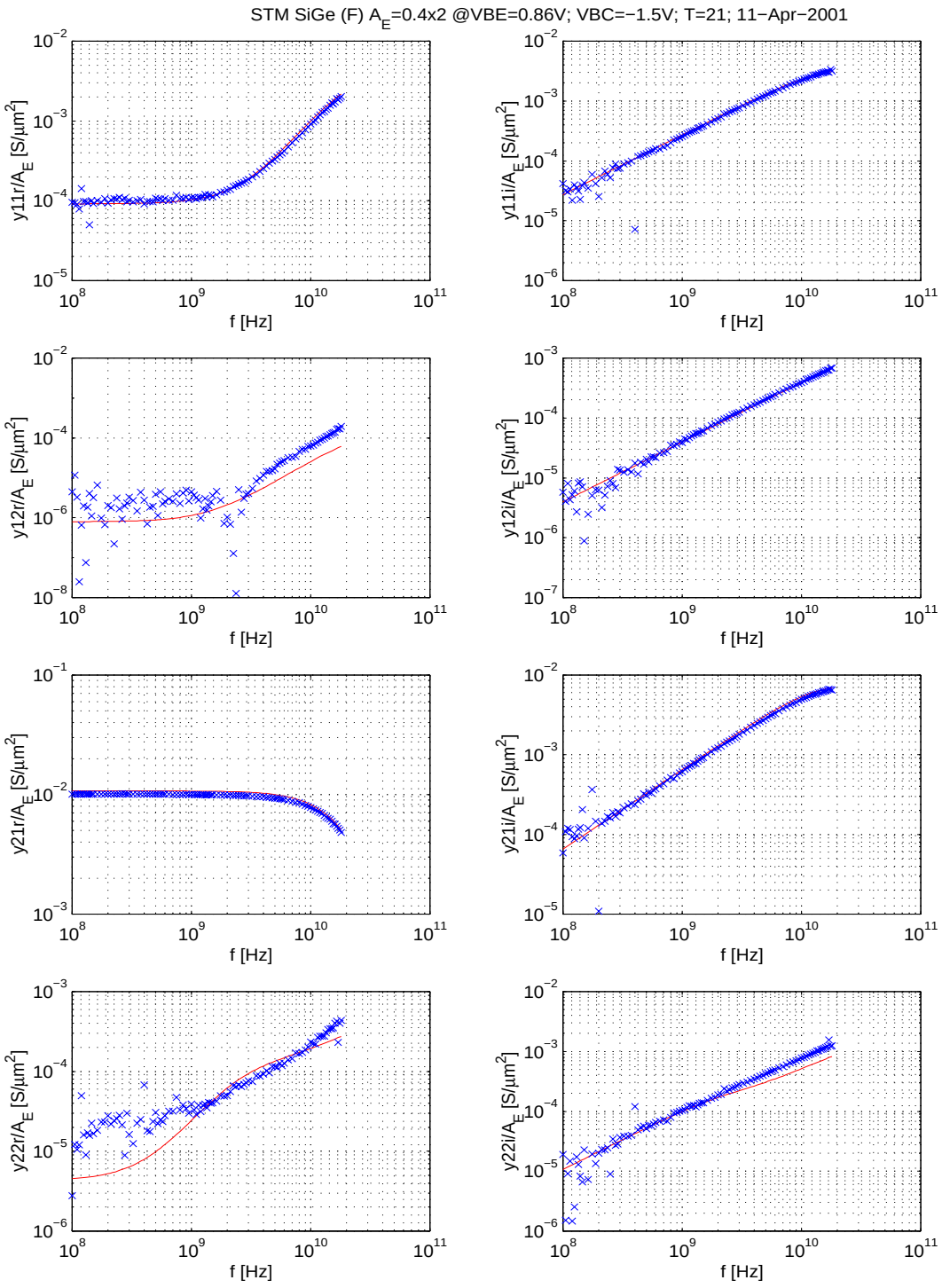

Fig. 1.3/8: Frequency dependent y-parameters at V_{BC} = -1.5V and I_C/A_E below peak f_T.

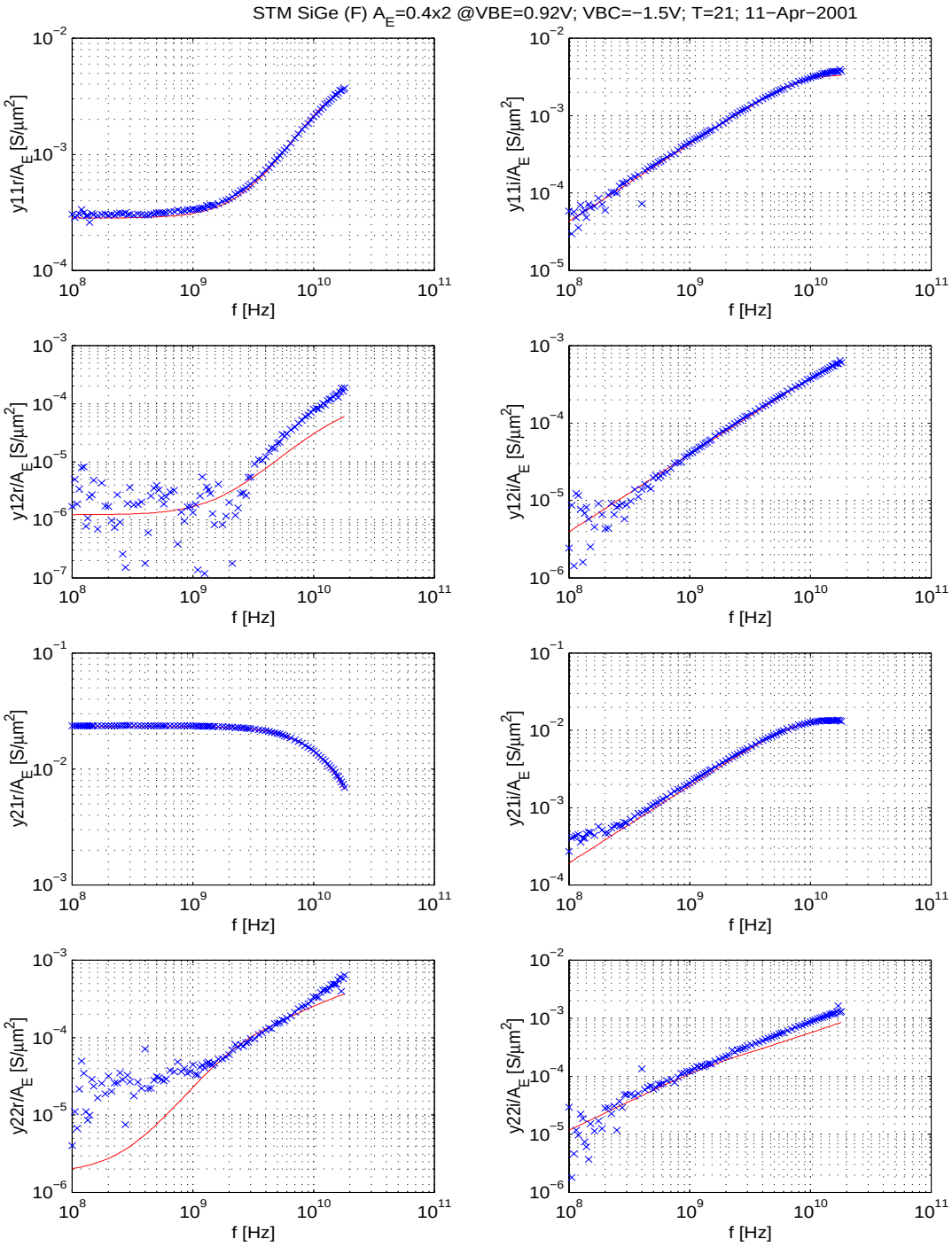

Fig. 1.3/9: Frequency dependent y-parameters at V_{BC} = -1.5V and I_C/A_E at peak f_T. 10E-15

```
 '*'  HICUM / LEVEL2  AC-Set
 'MODQ' 'Tref' 1
  &HICUM2 c10=6.4E-33     qp0=2.00E-15     ich=4.0E-03     hfc= 0.01
        hfe= 1.00        hjci= 0.355       hjei= 1.00       alit=0.450
        cjei0=3.36E-15   vdei=0.940       zei=0.500        aljei= 3.00
        cjci0=3.69E-16   vdci=0.750       zci=0.400        vptci=1.00E+02
        t0=2.11E-12      dt0h= 9.000E-13  tbvl=1.200E-12   tef0=1.10E-13
        gtfe=  1.00      thcs=1.20E-10    alhc= 0.099      fthc= 0.800
        alqf=0.225
        rci0=1.95E+02    vlim= 0.532      vpt=  4.65       vces= 0.100
        tr=0.00E+00
        ibeis=8.2E-21    mbei=1.0000      ireis=3.00E-16   mrei=2.0000
        ibcis=1.00E-30   mbci=1.0240
        favl= 3.610      qavl=4.85E-15
        rbi0= 360.00     fdqr0=0.200      fgeo=0.8160      fqi=1.0000
        fcrbi=0.00
        latb=5.210E+00   latl=1.040
        cjep0=2.03E-15   vdep=0.960       zep=0.437        aljep= 3.00
        ibeps=1.00E-30   mbep=1.0110      ireps=1.00E-30   mrep=2.0000
        ibets=0.00E+00   abet=  0.00
        cjcx0=6.52E-15   vdcx=0.850       zcx=0.401        vptcx=3.00E+00
        ccox=1.77E-15    fbc=0.229
        ibcxs=2.37E-18   mbcx=1.0240
        ceox=6.17E-16    rbx=  90.00      re= 21.000       rcx=  30.00
        itss=1.00E-30    msf=1.000        tsf=0.00E+00
        iscs=1.00E-30    msc=1.000
        cjs0=1.40E-14    vds=1.284        zs=0.432         vpts=1.00E+02
        rsu=    0.0      csu=0.00E+00
        kf=0.00E+00      af=1.00E+00
        vgb= 1.170       alb=-7.00E-03    alt0= 0.00E+00   kt0= 0.00E+00
        zetaci=  1.630   alvs=1.00E-03    alces=4.00E-04   zetarbi=  0.900
        zetarbx=  0.150  zetarcx=  0.280  zetare= -1.000
        alfav=8.25E-05   alqav=1.96E-02
        rth= 1600.00     cth=0.00E+00  &end
```

Fig. 1.3/10: Set of model parameters for the AC measurement based comparison (DEVICE).

1.4 Results for the DC measurement data

Figures 1.4/1 to 1.4/7 contain a comparison between model (solid lines) and measurements (symbols). These DC data cover a larger bias range towards *very low* current densities and contain, in contrast to the data from AC measurements, no information on V_{BC} = 0.5V. For the comparison, most model parameters (cf. Fig. 1.4/8) were left unchanged from the previous ("AC") values, except the ones modeling the various base current components and the avalanche current, for which the absolute measured data also seem to be different. In general, similar agreement is obtained for the same characteristics that were already compared for the data set from AC measurements. This also holds for the bias region at very low current densities. A comment on the DC current gain B, which is - like the I-V_{BE} characteristics - of little use for high-speed digital applications, but can be of (some) importance for RF circuit design: the observed deviations in B at high current densities beyond peak f_T can be caused by uncertainties in (a) Q_{p0} (and geometry partitioning of depletion charges), (b) self heating and temperature coefficients, and (c) geometry partitioning of the minority charge and associated current dependence.

In addition to the usual DC characteristics, several low-frequency derivatives, i.e. (normalized) conductances, are shown.

- In Fig. 1.4/2, the output conductance:

$$g_o = \left.\frac{dI_C}{dV_{CE}}\right|_{I_B} . \tag{1.4.0-1}$$

  The agreement is fairly good at low voltages V_{CE}, while at higher voltages certain deviations are observable, which are believed mainly to be due to (a) insufficient knowledge about the voltage dependence of the internal BC junction capacitance (cannot be extracted from a single device) and other relevant parameters, and (b) the weak avalanche model that does not take into account the breakdown mechanism at high current densities.

- In Fig. 1.4/4, the normalized transconductance:

$$\frac{g_m}{I_C} = \frac{1}{I_C}\left.\frac{dI_C}{dV_{BE}}\right|_{V_{BC}} . \tag{1.4.0-2}$$

  The observed deviations might in part be due to a slightly too low simulation temperature compared to the not exactly known measurement temperature. Other causes are believed to be insufficient information on the partitioning of internal and peripheral base emitter capacitance which cannot be obtained from a single device.

- In Fig. 1.4/6, the normalized input conductance:

$$\frac{g_{BE}}{I_B} = \frac{1}{I_B}\left.\frac{dI_B}{dV_{BE}}\right|_{V_{BC}} \tag{1.4.0-3}$$

The deviations at very high current densities can be due to the unknown partitioning of various effects (as already discussed before) and would need further investigation. However, the importance of the above characteristic for circuit design is unclear.

All derivatives were obtained by numerical differentiation of either the linear (go) or log data (g_m, g_{BE}).

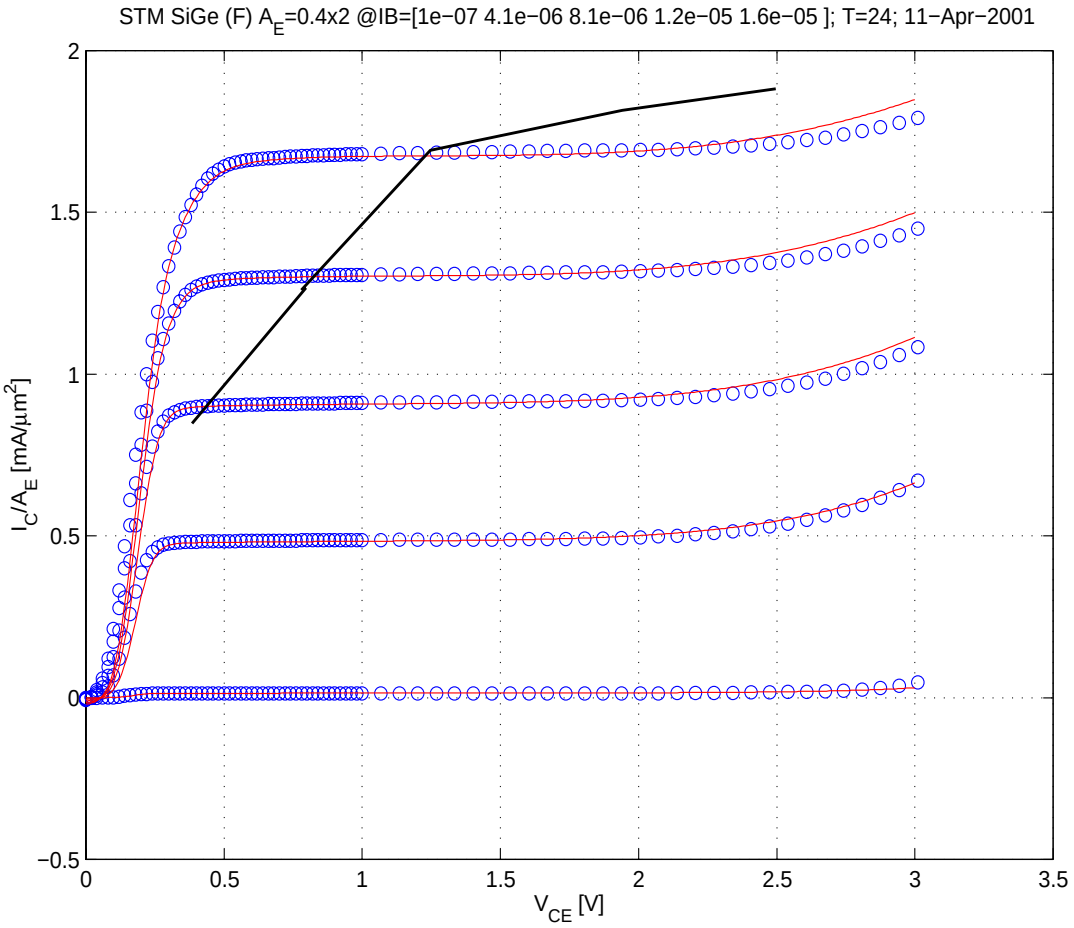

Fig. 1.4/1: Forward output characteristics with $I_B/\mu A$ = 0.1, 4.1, 8.1, 12.1, 16.1. Data source: DC measurements. A larger base current than 16.1 µA has not been available from measurements.
The additional curve indicates the current at which f_T peaks, assuming J_C values between about 0.8 and 2 mA/µm^2.

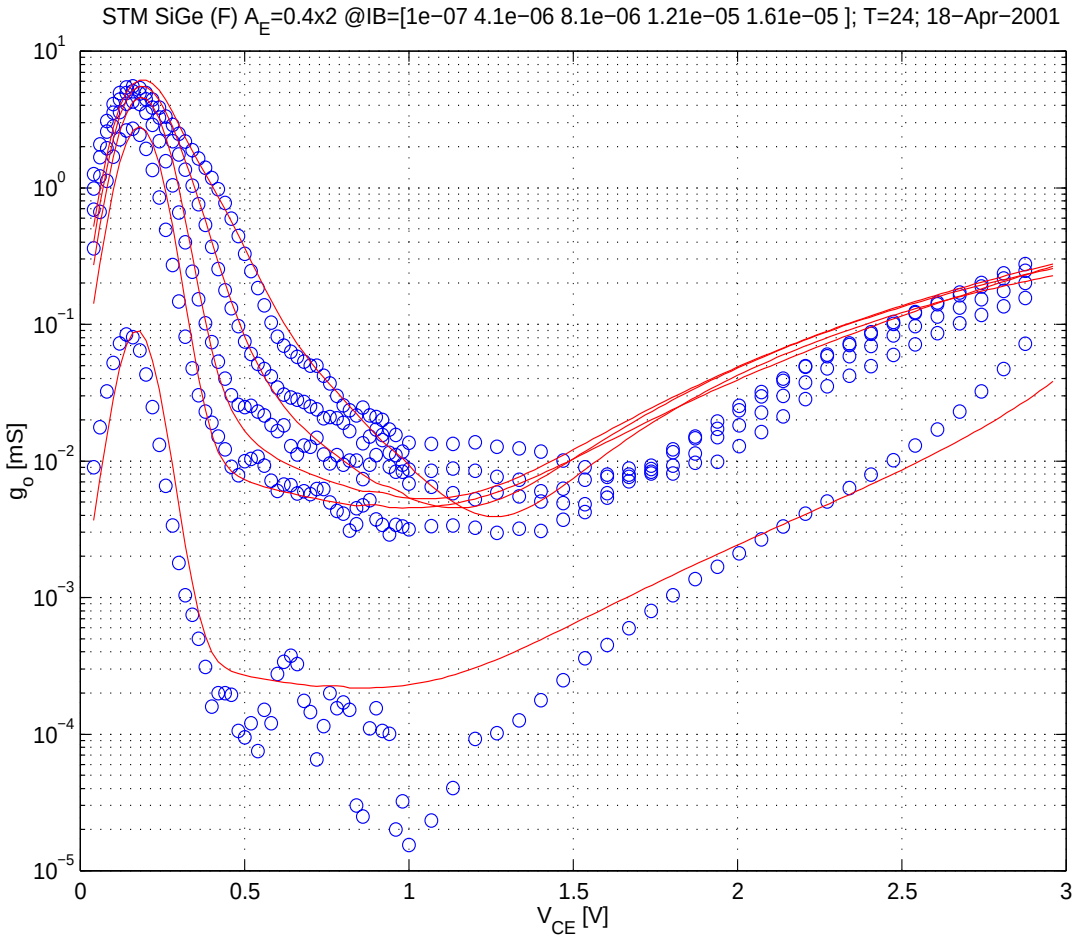

Fig. 1.4/2: Output conductance vs. V_{CE} for $I_B/\mu A$ = 0.1, 4.1, 8.1, 12.1, 16.1. Data source: DC measurements. The crossing of the conductance, which also occurs in measurement, can be caused by the competing effects of Early effect, weak avalanche and self-heating in combination with a negative TC of the current gain.

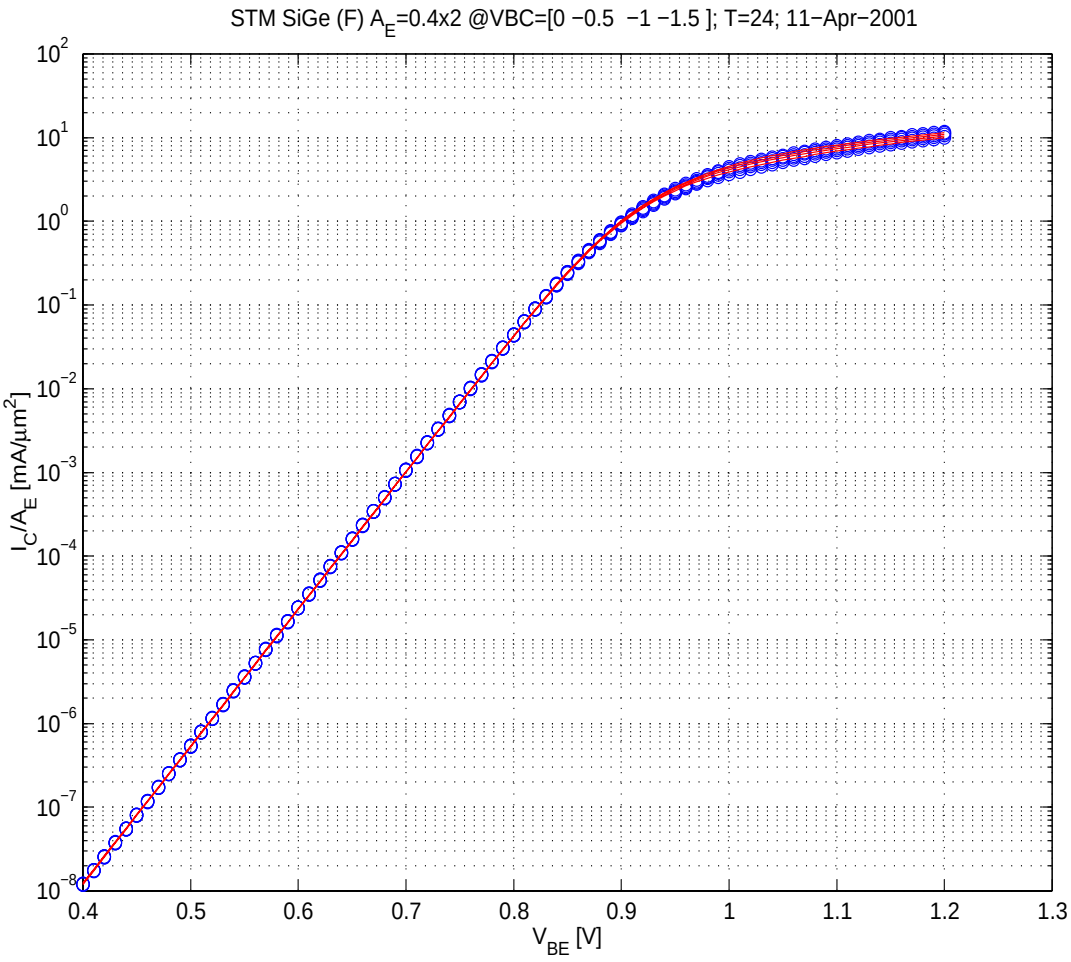

Fig. 1.4/3: Collector current density vs. V_{BE} for V_{BC}/V = 0, -0.5, -1, -1.5. Data source: DC measurements.

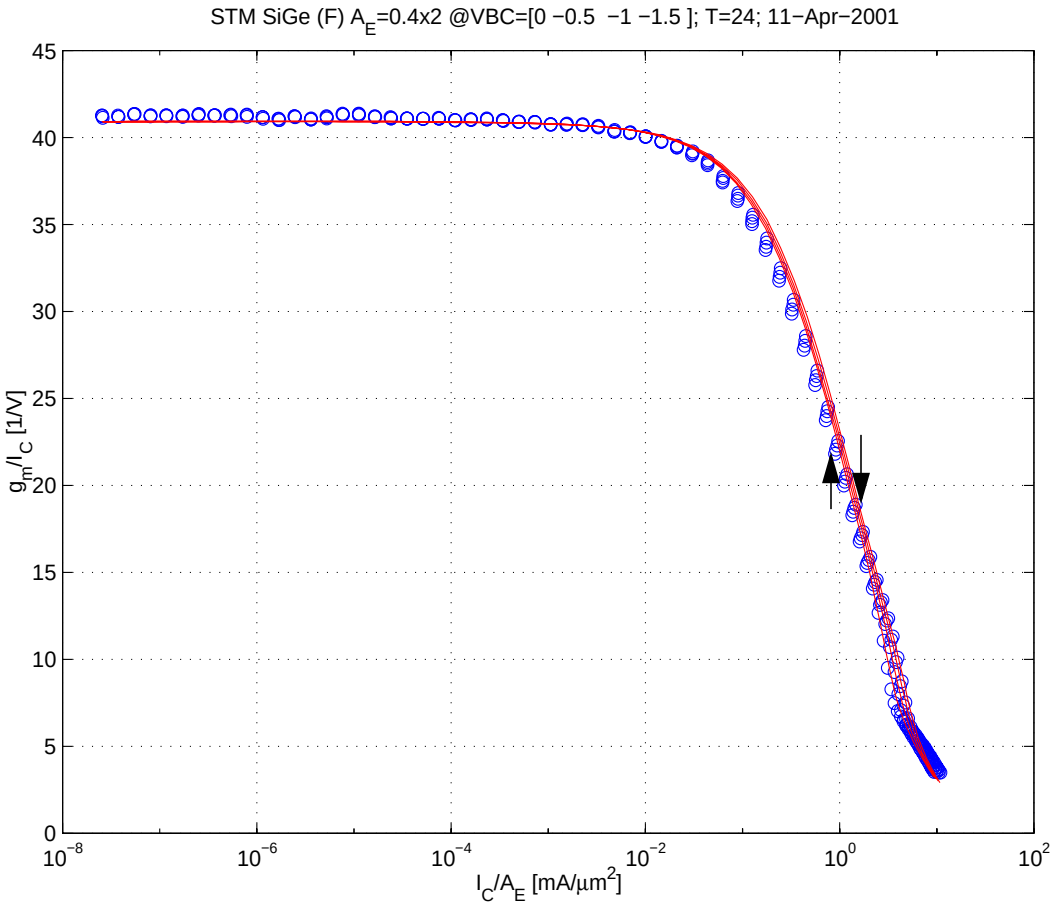

Fig. 1.4/4: Normalized low-frequency transconductance vs. collector current density;
V_{BC}/V = 0, -0.5, -1, -1.5. Data source: DC measurements.
The arrows indicate peak f_T for the lowest and highest V_{BC} value.

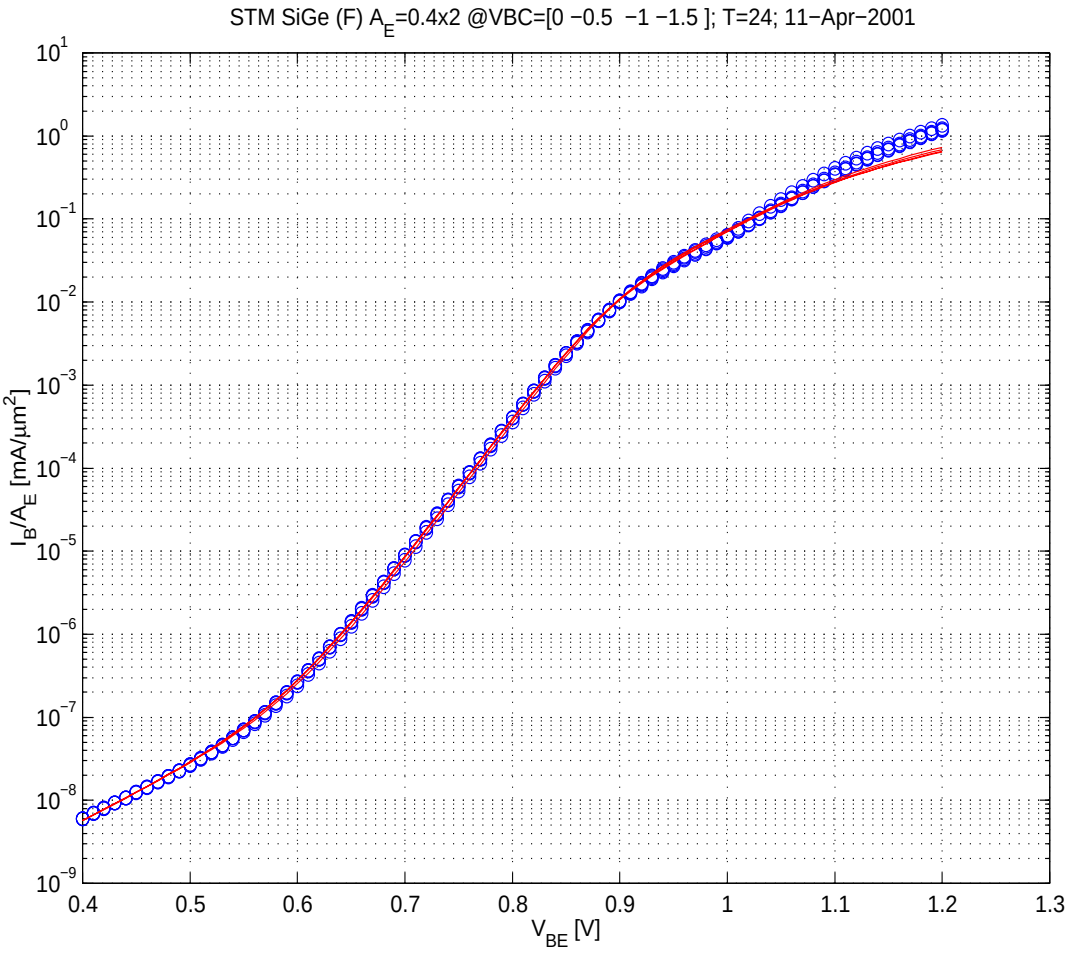

Fig. 1.4/5: Base current density vs. V_{BE} for V_{BC}/V = 0, -0.5, -1, -1.5. Data source: DC measurements.

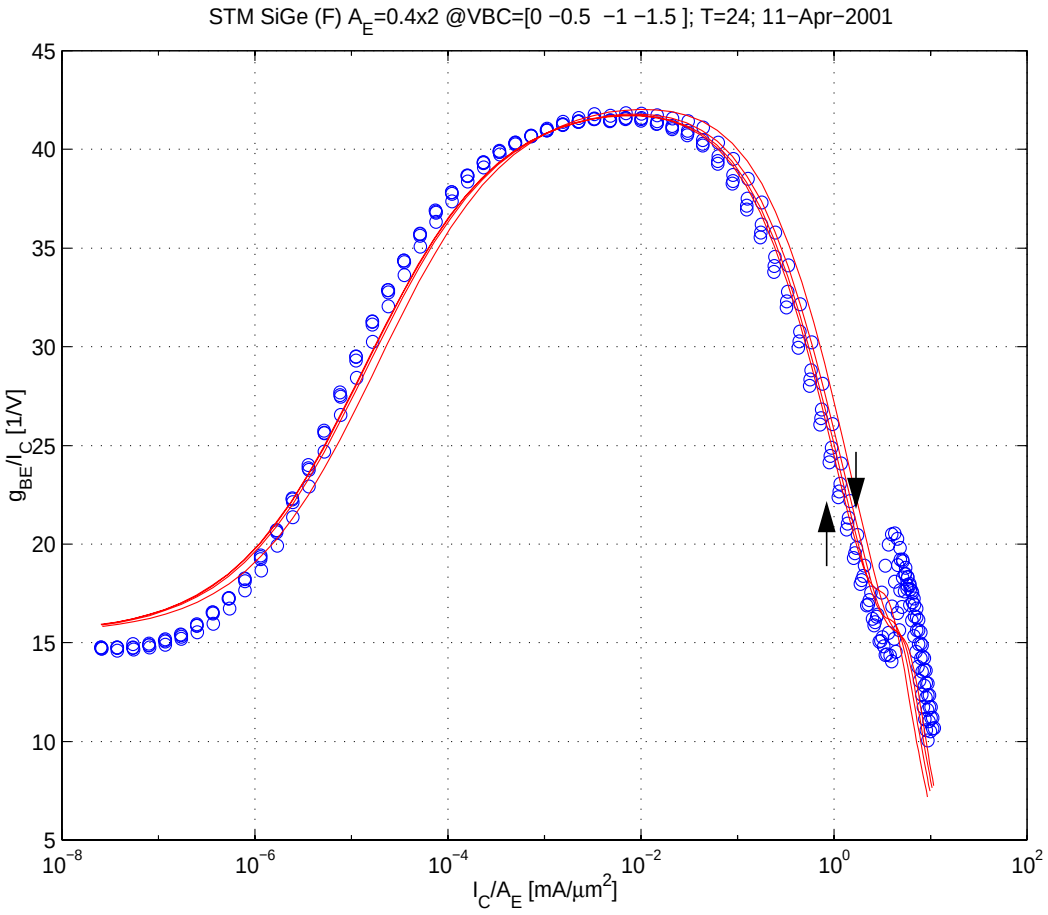

Fig. 1.4/6: Normalized low-frequency input conductance vs. collector current density;
V_{BC}/V = 0, -0.5, -1, -1.5. Data source: DC measurements.
The arrows indicate peak f_T for the lowest and highest V_{BC} value.

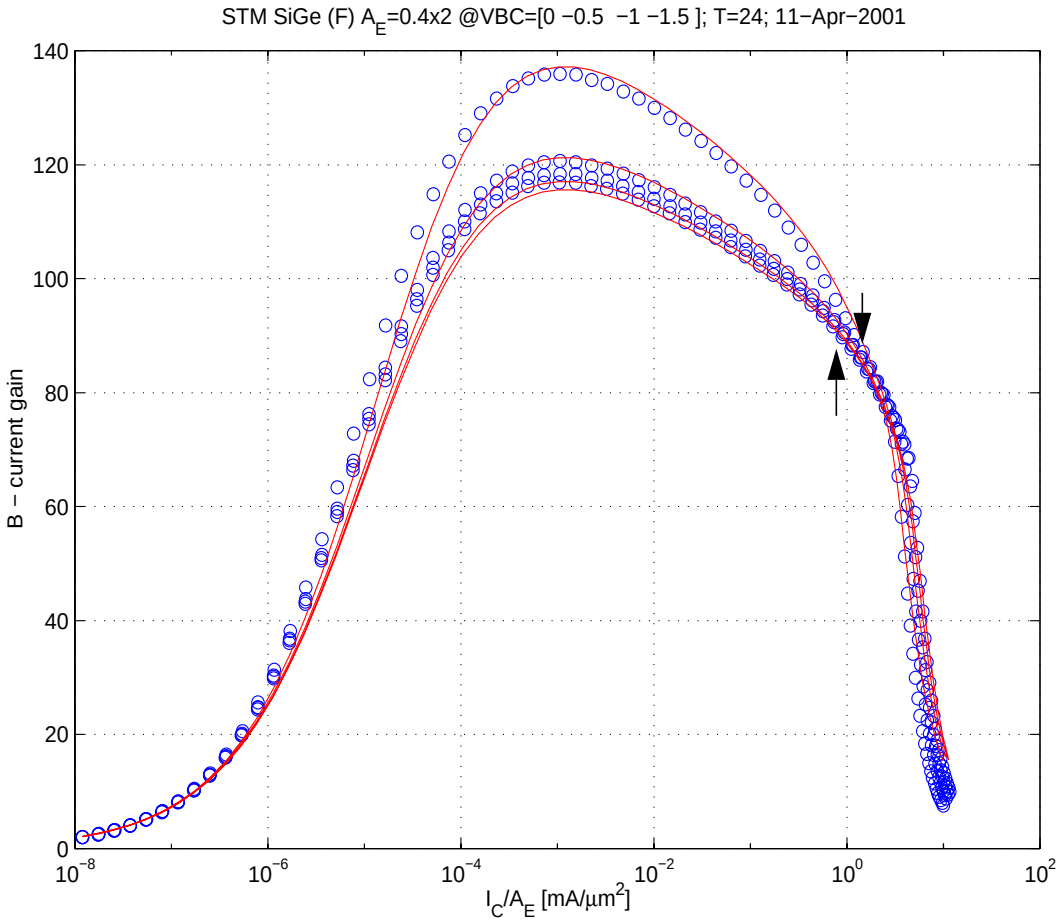

Fig. 1.4/7: DC current gain vs. collector current density for V_{BC}/V = 0.5, 0, -0.5, -1, -1.5; T = 23C. Data source: DC measurements. The arrows indicate peak f_T for the lowest and highest V_{BC} value.

```
'*'  HICUM / LEVEL2    DC-Set
'MODQ' 'Tref' 1
 &HICUM2 c10=3.50E-33     qp0=2.00E-15     ich=4.15E-03     hfc= 0.01
       hfe= 1.00       hjci= 0.3       hjei= 1.00       alit=0.450
       cjei0=3.36E-15   vdei=0.940       zei=0.500        aljei= 3.00
       cjci0=3.69E-16   vdci=0.750       zci=0.500        vptci=1.00E+02
       t0=1.90E-12      dt0h= 6.000E-19  tbvl=8.000E-19   tef0=1.00E-19
       gtfe=  1.00      thcs=2.00E-11    alhc= 0.200      fthc= 0.400
       alqf=0.225
       rci0=1.80E+02    vlim= 0.532      vpt=  3.20       vces= 0.100
       tr=0.00E+00
       ibeis=5.43E-21   mbei=1.0000      ireis=8.50E-15   mrei=2.5700
       ibcis=1.00E-30   mbci=1.0240
       favl= 6      qavl=4.30E-15
       rbi0= 360.00     fdqr0=0.200      fgeo=0.8160      fqi=1.0000
       fcrbi=0.00
       latb=5.210E+00   latl=1.040
       cjep0=2.03E-15   vdep=0.960       zep=0.437        aljep= 2.00
       ibeps=1.00E-30   mbep=1.0110      ireps=1.00E-30   mrep=2.0000
       ibets=0.00E+00   abet=  0.00
       cjcx0=7.53E-15   vdcx=0.635       zcx=0.240        vptcx=1.00E+02
       ccox=1.77E-15    fbc=0.229
       ibcxs=8.37E-18   mbcx=1.0240
       ceox=6.17E-16    rbx=  90.00      re= 21.000       rcx=  30.00
       itss=1.00E-30    msf=1.000        tsf=0.00E+00
       iscs=1.00E-30    msc=1.000
       cjs0=1.40E-14    vds=1.284        zs=0.432         vpts=1.00E+03
       rsu=    0.0      csu=0.00E+00
       kf=0.00E+00      af=1.00E+00
       vgb= 1.170       alb=-6.40E-03    alt0= 0.00E+00   kt0= 0.00E+00
       zetaci=  1.630   alvs=1.00E-03    alces=4.00E-04   zetarbi=  0.900
       zetarbx=  0.150  zetarcx=  0.280  zetare= -1.000
       alfav=8.25E-05   alqav=1.50E-02
       rth= 1600.00     cth=0.00E+00  &end
```

Fig. 1.4/8: Model parameter set (DEVICE) extracted from the DC measurements.